

## Coupled Conformational Equilibria in $\beta$ -Sheet Peptide–Dendron Conjugates

Hui Shao, Jeffrey W. Lockman, and Jon R. Parquette\*

Department of Chemistry, The Ohio State University, 100 West 18th Avenue Columbus, Ohio 43210

Received November 14, 2006; E-mail: parquett@chemistry.ohio-state.edu

The occurrence of dynamically correlated equilibria relating local and nonlocal structural elements in proteins greatly influences processes such as ligand binding, catalysis, allostery, and thermodynamic stability.<sup>1</sup> Related dynamics occurring within a single structural element mediates the chiral amplification exhibited by helical polymers, supramolecular assemblies, and dendrimers.<sup>2</sup> However, the design of synthetic systems displaying the hierarchical structural order present in natural systems remains a significant challenge. Progress toward this level of structural organization requires the ability to design conjugate structures that couple the equilibria of multiple, unique secondary structural elements over long distances. We recently reported a short-range example of hierarchical organization wherein coupled equilibria relating the terminal pentaethyleneglycol chain conformations with dendron helicity induced a solvent-mediated  $M \rightarrow P$  helical inversion.<sup>3</sup> Similarly, chiral communication between a helical polymer<sup>4</sup> or dipeptide<sup>5</sup> backbone and appended dendrons within liquid crystalline assemblies represents progress toward this goal. In this work, we report the  $\alpha$ -helix to  $\beta$ -sheet conformational transition of an intrinsically  $\alpha$ -helical alanine-rich sequence that is induced by hydrophobic dendron packing in water. The chiral communication from the peptide backbone to the dendron helicity that emerges in the  $\beta$ -sheet form reveals a synergistic coupling of the conformations of both structural elements.

A series of peptide–dendron conjugates<sup>6</sup> were designed to determine the structural features necessary to correlate the peptide and dendron secondary structures. We reasoned that a construct that coupled peptide folding with dendron packing would mediate efficient chiral communication. Dendrons were appended to an  $\alpha$ -helical peptide backbone in an effort to position them along one face of the helix, separated by one helical turn (i.e., at the  $i$  and  $i + 4$  positions). This arrangement would stabilize the  $\alpha$ -helix, similar to the stabilization induced by placing hydrophobic groups at these positions,<sup>7</sup> and would concomitantly pack the dendrons in a manner that amplifies the dendron helical bias.<sup>8</sup> In this work, we found this process actually operative within a  $\beta$ -sheet context wherein hydrophobic dendron packing induces a conversion from an  $\alpha$ -helical to a  $\beta$ -sheet structure that displays strong chiral communication lacking in the  $\alpha$ -helical form (Figures 1 and 2).

In order to explore the envisaged  $\alpha$ -helical construct, the peptide–dendron conjugate was based on an alanine-rich peptide sequence, due to the high helix propensity of alanine.<sup>9</sup> Two dendron-modified alanine residues ( $A^D$ ), displaying achiral terminal tetraethylene glycol chains to impart water solubility, were incorporated within the peptide sequence. The interaction between the dendrons was explored in conjugates by progressively increasing the inter-dendron spacing from  $i, i + 4$  (**2**) to  $i, i + 11$  (**9**) (Table 1). The peptides were assembled using Fmoc/*t*-Bu solid-phase peptide synthesis on rink amide resin (Supporting Information).

The dendron and peptide conformational states were independently measured using circular dichroism (CD) and FTIR spectroscopy. The peptide conformation was monitored by CD at 222 nm, a region where the dendrons tend to have weak Cotton effects,

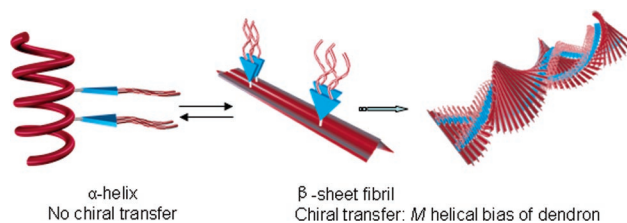


**Figure 1.** Notional depiction of dendron packing in  $\alpha$ -helical and  $\beta$ -sheet structural forms.

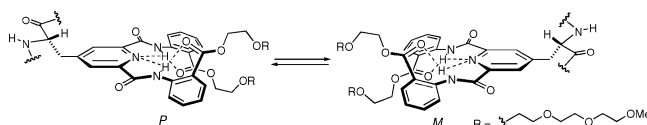


**Figure 2.** Helical conformational equilibria of dendron-modified alanine residue ( $A^D$ ) within the peptide–dendron conjugate.

**Table 1.** Peptide–Dendron Sequences

peptide	dendrons	sequence
<b>1</b>	control	Ac–AAAAKAAA KAAAAAYA–NH <sub>2</sub>
<b>2</b>	$i, i + 4$	Ac–AAA <sup>D</sup> AKAAA <sup>D</sup> AAKAAAAAYA–NH <sub>2</sub>
<b>3</b>	$i, i + 5$	Ac–AAA <sup>D</sup> AKAAA <sup>D</sup> AKAAAAAYA–NH <sub>2</sub>
<b>4</b>	$i, i + 6$	Ac–AAA <sup>D</sup> AKAAA <sup>D</sup> PKAAAAAYA–NH <sub>2</sub>
<b>5</b>	$i, i + 7$	Ac–AAA <sup>D</sup> AAKAAAA <sup>D</sup> KAAAAAYA–NH <sub>2</sub>
<b>6</b>	$i, i + 8$	Ac–AAA <sup>D</sup> AKAAAAA <sup>D</sup> KAAAAAYA–NH <sub>2</sub>
<b>7</b>	$i, i + 9$	Ac–AAA <sup>D</sup> AKAAAAA <sup>D</sup> KAAAYA–NH <sub>2</sub>
<b>8</b>	$i, i + 10$	Ac–AAA <sup>D</sup> AKAAAAA <sup>D</sup> KAAA <sup>D</sup> PAYA–NH <sub>2</sub>
<b>9</b>	$i, i + 11$	Ac–AAA <sup>D</sup> AKAAAAA <sup>D</sup> KAAA <sup>D</sup> PYA–NH <sub>2</sub>

whereas the helical bias in the dendrons was observed by the excitonic couplet centered at 316 nm. Accordingly, the CD spectra of the peptides were recorded as a function of added 2,2,2-trifluoroethanol (TFE) in 20 mM sodium phosphate buffer (10 mM NaCl, pH 7.0) (PBS) at 25 °C (Supporting Information). All peptide–dendron conjugates except **4** ( $i, i + 6$ ) and **8** ( $i, i + 10$ ) afforded  $\alpha$ -helical structures that increased in helicity at higher TFE/PBS ratios, exhibiting maximal  $\alpha$ -helical contents of ca. 50% at 60% TFE/PBS, slightly lower than that of the control peptide **1**.

Peptide–dendrons **4** ( $i, i + 6$ ) and **8** ( $i, i + 10$ ) adopted  $\beta$ -sheet structures in PBS, as evidenced by the peaks at 218 nm in the CD spectra that became  $\alpha$ -helical at >20% TFE/PBS (Figure 3A and Supporting Information). The presence of antiparallel  $\beta$ -sheet structures in D<sub>2</sub>O and  $\alpha$ -helical forms in TFE were similarly indicated by FTIR<sup>10</sup> (Figure 3B). Deconvolution of the spectra provided an  $\alpha$ -helix/ $\beta$ -sheet/random coil distribution for **4** and **8** of 45:8:47 and 52:8:40 in TFE and 5:90:5 and 2:95:3 in D<sub>2</sub>O, respectively. The  $\alpha$ -helical content values determined by FTIR compared favorably with those determined by CD spectroscopy (**4**: 12(D<sub>2</sub>O)/46(TFE); **8**: 8(D<sub>2</sub>O)/50 (TFE)).

Intra- and interstrand interactions among laterally and diagonally paired hydrophobic side chains contribute significantly to the stability of  $\beta$ -sheet structures.<sup>11</sup> Likewise, intermolecular hydrophobic association of the dendritic side chains likely drives the  $\alpha$ -helix to  $\beta$ -sheet interconversion going from TFE to water.

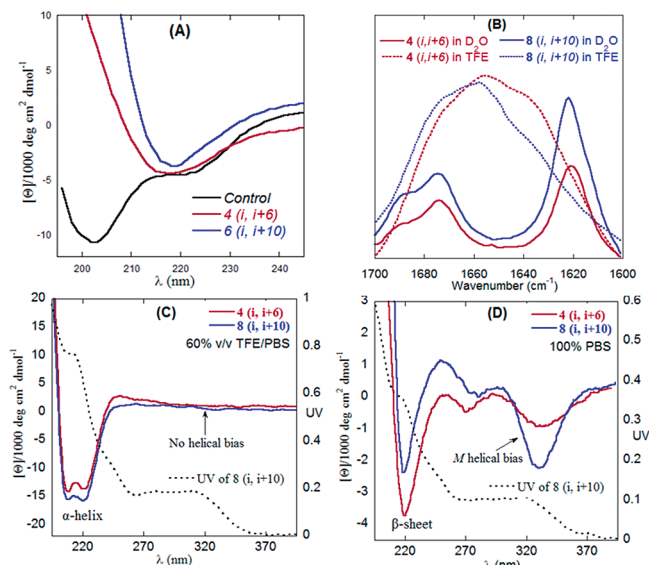


**Figure 3.** (A) CD spectra of peptides **4** (*i, i + 6*), **8** (*i, i + 10*), and **1** (control) ( $50 \mu\text{M}$  in PBS). (B) Amide I region of FTIR spectra of **4** and **8** in  $\text{D}_2\text{O}$  and TFE ( $10 \text{ mg/mL}$ ). (C) CD spectra of **4** and **8**, and UV-vis spectrum of **8** in 60% v/v TFE/PBS ( $50 \mu\text{M}$ ). (D) CD spectra of **4** and **8**, and UV-vis spectrum of **8** in PBS ( $50 \mu\text{M}$ ).

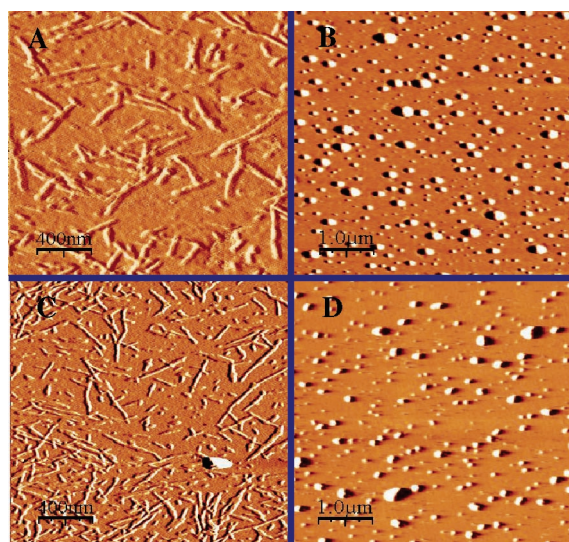


**Figure 4.** Tapping-mode AFM images of **4** (*i, i + 6*) and **8** (*i, i + 10*) peptide conjugates. (A) **4** in PBS ( $10 \mu\text{M}$ ); (B) **4** in 60% v/v TFE/PBS ( $5 \mu\text{M}$ ); (C) **8** in PBS ( $10 \mu\text{M}$ ); (D) **8** in 60% v/v TFE/PBS ( $5 \mu\text{M}$ ).

Although the potential for fibrillogenesis exists for all proteins,<sup>12</sup> alanine-rich peptides generally adopt  $\alpha$ -helical conformations that increase in stability with increasing TFE (i.e., peptide **1**).<sup>9</sup> The capability of these sequences to adopt  $\beta$ -sheet structures at very high concentrations ( $10 \text{ mM}$ ) was recently observed for the sequence  $\text{Ac}-(\text{AAKA})_4-\text{NH}_2$ .<sup>13</sup> In contrast, peptide-dendrons **4** and **8** adopt stable  $\beta$ -sheet conformations at  $50 \mu\text{M}$  by CD. Furthermore, atomic force microscopy (AFM) of both peptides revealed amyloid-like nanofibrils in PBS buffer at  $10 \mu\text{M}$ , whereas in 60% TFE/PBS, globular aggregates were observed (Figure 4). Additionally, **4** forms a hydrogel in water at concentrations as low as  $1.7 \text{ mM}$ .<sup>14</sup> The dimensions of the fibrils of both peptides were similar to that of natural amyloid fibers,<sup>15</sup> and some fibrils exhibited a left-handed twist that repeats along the fiber length (see Supporting Information).<sup>16</sup>

The intermolecular dendron association that stabilizes the  $\beta$ -sheet structure simultaneously promotes the transfer of chiral conforma-

tional information from the peptide to the dendron. Accordingly, an intense negative couplet centered at ca.  $316 \text{ nm}$  emerges for the  $\beta$ -sheet forms of **4** and **8** in PBS. The couplet disappears in 60% TFE/PBS when the peptides adopt  $\alpha$ -helical structures and is absent in PBS and 60% TFE/PBS for the other peptides (Figure 2C,D). The presence of the negative couplet indicates an *M*-type helical bias relating the anthranilate chromophores of the dendrons (Figure 2).<sup>8</sup> The development of a helical bias requires a formal transfer of chirality from the focal peptide sequence to the achiral anthranilate termini. It is noteworthy that we have found this transfer of chirality difficult in prior studies due to the lack of any apparent steric interactions capable of communicating focal point chirality with the dendron termini.<sup>8d</sup> The lower efficiency of chiral communication in **4** compared with that in **8**, as evidenced by a lower intensity couplet, likely emanates from subtle differences in the nature and extent of intermolecular dendron packing.

These studies support the supposition that chiral communication between the peptide and dendron structural elements occurs most efficiently in constructs that couple peptide folding with dendron packing. In this case, dendron association perturbs the intrinsic  $\alpha$ -helical preference of alanine-rich sequences and enforces  $\beta$ -sheet formation. Accordingly, the intended conformational synergism occurs to a much greater extent within an aggregated  $\beta$ -sheet motif than within an  $\alpha$ -helical context.

**Acknowledgment.** This work was supported by the National Science Foundation (CHE-0239871).

**Supporting Information Available:** Experimental, FTIR, AFM, CD, and MS data for the studied peptides. This material is available free of charge via the Internet at <http://pubs.acs.org>.

## References

- Boehr, D. D.; Dyson, H. J.; Wright, P. E. *Chem. Rev.* **2006**, *106*, 3055–3079.
- Lockman, J. W.; Paul, N. M.; Parquette, J. R. *Prog. Polym. Sci.* **2005**, *30*, 423–452.
- Hofacker, A. L.; Parquette, J. R. *Angew. Chem., Int. Ed.* **2005**, *44*, 1053–1057.
- Percec, V.; Rudick, J. G.; Peterca, M.; Wagner, M.; Obata, M.; Mitchell, C. M.; Cho, W.-D.; Balagurusamy, V. S. K.; Heiney, P. A. *J. Am. Chem. Soc.* **2005**, *127*, 15257–15264.
- Peterca, M.; Percec, V.; Dulcey, A. E.; Nummelin, S.; Korey, S.; Ilies, M.; Heiney, P. A. *J. Am. Chem. Soc.* **2006**, *128*, 6713–6720.
- (a) Lee, C. C.; Frechet, J. M. J. *Macromolecules* **2006**, *39*, 476–481. (b) Wathier, M.; Johnson, C. S.; Kim, T.; Grinstaff, M. W. *Bioconjugate Chem.* **2006**, *17*, 873–876. (c) Delort, E.; Nguyen-Trung, N.-Q.; Darbre, T.; Reymond, J.-L. *J. Org. Chem.* **2006**, *71*, 4468–4480. (d) Kim, K. T.; Park, C.; Kim, C.; Winnik, M. A.; Manners, I. *Chem. Commun.* **2006**, 1372–1374.
- Albert, J. S.; Hamilton, A. D. *Biochemistry* **1995**, *34*, 984–990.
- (a) Huang, B.; Prantil, M. A.; Gustafson, T. L.; Parquette, J. R. *J. Am. Chem. Soc.* **2003**, *125*, 14518–14530. (b) Huang, B.; Parquette, J. R. *J. Am. Chem. Soc.* **2001**, *123*, 2689–2690. (c) Recker, J.; Tomcik, D. J.; Parquette, J. R. *J. Am. Chem. Soc.* **2000**, *122*, 10298–10307. (d) Gandhi, P.; Huang, B.; Gallucci, J. C.; Parquette, J. R. *Org. Lett.* **2001**, *3*, 3129–3132.
- Marqusee, S.; Robbins, V. H.; Baldwin, R. L. *Proc. Natl. Acad. Sci. U.S.A.* **1989**, *86*, 5286–5290.
- Goormaghtigh, E.; De Meutter, J.; Szoka, F.; Cabiaux, V.; Parente, R. A.; Ruysschaert, J. M. *Eur. J. Biochem.* **1991**, *195*, 421–429.
- (a) Griffiths-Jones, S. R.; Searle, M. S. *J. Am. Chem. Soc.* **2000**, *122*, 8350–8356. (b) Syud, F. A.; Stanger, H. E.; Gellman, S. H. *J. Am. Chem. Soc.* **2001**, *123*, 8667–8677. (c) Phillips, S. T.; Piersanti, G.; Bartlett, P. A. *Proc. Natl. Acad. Sci. U.S.A.* **2005**, *102*, 13737–13742.
- MacPhee, C. E.; Dobson, C. M. *J. Am. Chem. Soc.* **2000**, *122*, 12707–12713.
- Measey, T. J.; Schweitzer-Stenner, R. *J. Am. Chem. Soc.* **2006**, *128*, 13324–13325.
- Pochan, D. J.; Schneider, J. P.; Kretsinger, J.; Ozbas, B.; Rajagopal, K.; Haines, L. *J. Am. Chem. Soc.* **2003**, *125*, 11802–11803.
- Khurana, R.; Ionescu-Zanetti, C.; Pope, M.; Li, J.; Nielson, L.; Ramirez-Alvarado, M.; Regan, L.; Fink, A. L.; Carter, S. A. *Biophys. J.* **2003**, *85*, 1135–1144.
- Marini, D. M.; Hwang, W.; Lauffenburger, D. A.; Zhang, S.; Kamm, R. D. *Nano Lett.* **2002**, *2*, 295–299.

JA068154N